Anomalous X-ray scattering reveals the role of constituent elements in $Ge_2Sb_2Te_5$

S. Kohara[a], K. Ohara[a], L. Temleitner[a,b], K. Sugimoto[a], T. Matsunaga[c], L. Pusztai[b], M. Itou[a], H. Ohsumi[d], R. Kojima[c], N. Yamada[c], T. Usuki[e], A. Fujiwara[a], and M. Takata[a,d]

[a]JASRI/ SPring-8, 1-1-1 Kouto, Sayo-cho, Sayo-gun, Hyogo 679-5198, Japan
[b]Wigner Research Centre for Physics, Hungarian Academy of Sciences, H-1525 Budapest, P. O. Box 49, Hungary
[c]Panasonic Corporation, 3-1-1 Yagumo-Nakamachi, Moriguchi, Osaka 570-8501, Japan
[d]RIKEN, 1-1-1 Kouto, Sayo-cho, Sayo-gun, Hyogo 679-5148, Japan
[e]Department of Material and Biological Chemistry, Faculty of Science, Yamagata University, 1-4-12 Koshirakawa, Yamagata 990-8560, Japan

ABSTRACT

We succeeded, for the first time, in measuring anomalous X-ray diffraction data on amorphous $Ge_2Sb_2Te_5$ (GST), which allows us to distinguish Sb- and Te-related atomic correlations. Furthermore, we have performed high-energy X-ray diffraction measurements on crystalline GST and applied reverse Monte Carlo structural modeling, in combination with density functional theory-molecular dynamics simulation, to both experimental data. We found that germanium and tellurium atoms form a "core" Ge-Te network associated with the formation of fourfold rings, which rings can be recognized as crystalline nuclei. It is also suggested that the Ge-Te network can stabilize the amorphous phase at room temperature and that this network can persist in the crystalline phase. On the other hand, antimony does not contribute to ring formation but constitutes a "pseudo" network with tellurium, in which the characteristic Sb–Te distance is somewhat longer than the covalent Sb–Te bond distance. This suggests that the Sb-Te pseudo network may act as a precursor to forming critical nuclei during the crystallization process. The findings indicate that the Ge-Te core network is responsible for the outstanding stability and rapid phase change of the amorphous phase while the Sb-Te pseudo network is responsible for triggering critical nucleation.

INTRODUCTION

Chalcogenide phase-change (PC) materials have been used in rewritable storage media, digital versatile disc – random access memory (DVD-RAM), DVD re-writable (DVD-RW), Blu-ray disc–rewritable (BD-RE) and non-volatile memory such as phase-change random access memory (PC-RAM). Numerous studies on the structure of amorphous (a-) $Ge_2Sb_2Te_5$ (GST) [1)] have been reported early in the last decade using experimental methods such as extended X-ray absorption fine-structure spectroscopy (EXAFS), high-energy X-ray diffraction (HEXRD) with the aid of reverse Monte Carlo (RMC) simulation, hard X-ray photoemission spectroscopy (HXPS) and theoretical methods. Thus the structure of a-GST and its relationship with rapid phase change is gradually being uncovered; the most recent results are reviewed in ref. 2. For understanding the role of each element beyond the nearest coordination distance, with a special focus on the question of why a-GST is stable at room temperature for a long time despite the fact that it can rapidly transform to the crystalline phase, we performed anomalous X-ray scattering (AXS) measurements at the Sb and Te K edges. These experiments can provide information concerning the local environment of Sb and Te atoms beyond the nearest neighbour distance, in contrast to EXAFS. Furthermore, RMC modelling has been applied to AXS and HEXRD datasets on a-GST, while only to the latter for crystal (c-) GST, with a special focus on the connectivity of Ge-Te units and Sb-Te units beyond the nearest coordination distance.[3)]

EXPERIMENTS

Details of sample preparation are described in ref. 4.

The high-energy X-ray diffraction experiment on c-GST was carried out at room temperature at the SPring-8 high-energy XRD beamline BL04B2[5] using a two-axis diffractometer. The incident X-ray energy was 61.6 keV.

Room temperature anomalous X-ray scattering measurements on a-GST were carried out at the SPring-8 single crystal structure analysis beamline BL02B1 using a 4-circle diffractometer. The AXS measurements were performed at 4 energies, 30.172 keV (Sb far edge), 30.422 keV (Sb near edge), 31.500 keV (Te far edge), and 31.750 keV (Te near edge).

RMC simulation on a-GST was carried out by starting from an atomic configuration obtained by RMC/density functional (DF)-molecular dynamics (MD) simulation (number of atoms: 460).[6] The experimental $\Delta S_{Sb}(Q)$ and $\Delta S_{Te}(Q)$ obtained from AXS measurement and the $S(Q)$ obtained from a high-energy X-ray diffraction measurement[7] were fitted simultaneously by employing the RMC++ code.[8] Modelling of c-GST was carried out using 7200 particles by the RMCPOW simulation code.[9]

RESULTS

Figure 1(a) shows total scattering structure factors, $S(Q)$, for c-GST and a-GST. The diffraction pattern of c-GST exhibits sharp Bragg peaks and a diffuse scattering pattern, while only the latter appears for a-GST. It is demonstrated that the $S(Q)$ of the RMC model (solid line) agrees well with experimental data (open circles). Differential structure factors, $\Delta S(Q)$, for Sb and Te obtained from AXS measurements are shown in Fig. 1(b). The differential structure factor of Sb, $\Delta S_{Sb}(Q)$ exhibits a peak at Q=1 Å^{-1}. This peak is also observed in HEXRD data for both phases (due to diffuse scattering present in c-GST), as shown in Fig. 1(a).

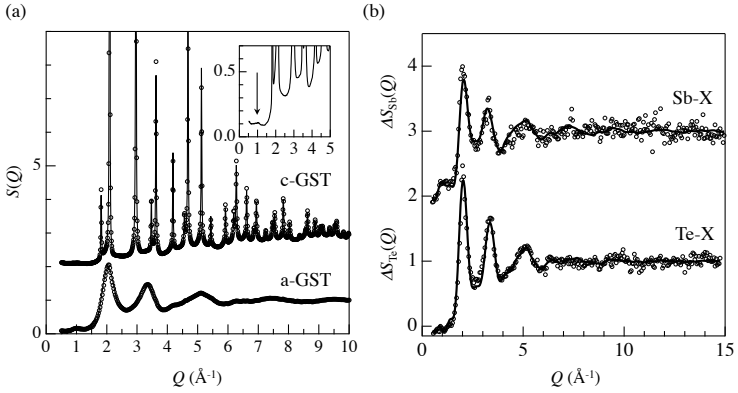

Fig. 1 Comparison between the experimental structure factors (open circle) and results of RMC modelling (solid line). (a) Total scattering data for c-GST and a-GST obtained by HEXRD measurements. The low Q part of c-GST data is enlarged in the inset. (b) $\Delta S(Q)$ for a-GST obtained by AXS measurements at Sb and Te K absorption edges.

For obtaining statistical structural features beyond the nearest coordination distance, ring statistics were calculated using a shortest path analysis.[10] As can be seen in Fig. 2(a), fourfold and sixfold rings consisting of '–(Ge, Sb)–Te–' units are dominant in c-GST. The existence of sixfold rings is due to the 20% vacancies on Ge/Sb mixing sites. As discussed in ref. 4, small '–(Ge, Sb)–Te–' rings such as fourfold, fivefold, and sixfold rings are dominant in a-GST. The numbers of rings consisting of '–Ge–Te–' units and of '–Sb–Te–' units in a-GST are shown in Fig. 2(b). Although the distribution of '–(Ge, Sb)–Te–' units has already been discussed in earlier studies,[2,4,6,7] we found for the first time that Ge-Te bonds form large numbers of fourfold and sixfold rings, while the contribution of Sb-Te bonds to the ring distribution is very small. Therefore it is suggested that the core network constructed by Ge-Te covalent bonds in a-GST is similar to that in c-GST, and that this core network plays an important role in stabilizing the amorphous phase at room temperature for long time.

To understand the atomic ordering by Ge-Te and Sb-Te bonds in detail, connectivities of atoms were calculated, by varying the maximum distance within which atomic pairs were considered to be connected. As can be seen in Fig. 3(a), about 60% of Ge-Te bonds up to 3.2 Å form a core network whereas Sb-Te bonds up to 3.2 Å do not form such a network. This distance corresponds to the covalent bond distance determined by DF-MD simulations.[6] Atomic configurations of Ge-Te and Sb-Te with bonds considered up to 3.2 Å are shown in Figs. 3(b) and 3(c), respectively. It can be clearly distinguished that Ge-Te bonds form a core network, which stabilizes the amorphous phase, whereas Sb-Te bonds do not. Furthermore it is evident that Ge-Te bonds form large fractions of fourfold (highlighted by blue) and sixfold (highlighted by light blue) rings, which can be recognized as crystalline nuclei as shown in Fig. 2d of ref. 4. On the other hand, about 70 % of the Sb-Te pairs form a pseudo network, as can be seen in Figs. 3(a) and 3(d), when bonds are considered up to 3.5 Å. In other words, the pseudo Sb-Te network becomes visible when we extend the correlation distance up to 3.5 Å, while such a feature cannot be observed for Ge-Te connectivities.

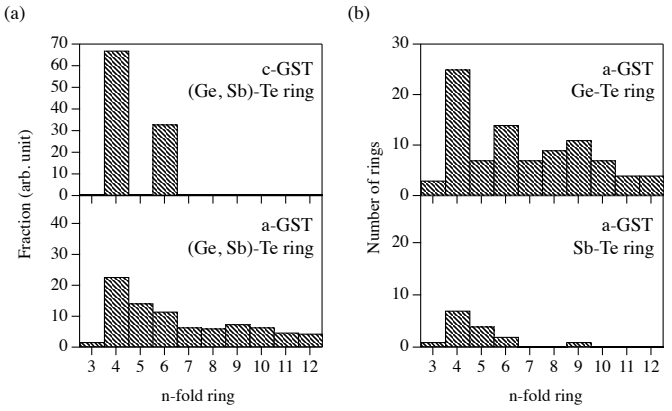

Fig. 2 Ring statistics for c-GST and a-GST calculated from the RMC models. (a) Normalized fraction of '–(Ge, Sb)–Te–' rings. (b) Numbers of '–Ge–Te– rings' and '–Sb–Te– rings' in a-GST. The total number of '–(Ge, Sb)–Te–' rings is normalized since the number of particles in the simulation box is not same for c-GST and a-GST.

On the basis of structural features in a-GST found above, we illustrate the phase-change scheme in Fig. 4. As highlighted by solid lines in Fig. 4(a), Ge-Te bonds significantly contribute to the network manifested by fourfold rings. Therefore Ge and Te can be recognized as network forming elements that stabilize the amorphous phase by strong Ge-Te covalent bonds[11] at room temperature for long time. The core Ge-Te network may remain in the crystalline-like phase, which feature explains rapid crystallization. As highlighted by dotted lines in Fig. 4(b), the Sb-Te correlations beyond the nearest coordination distance form a pseudo Sb-Te network. This unusual atomic ordering in terms of Sb-Te correlations can be ascribed to the combination of two positively charged atoms (Ge, -0.22 electrons; Sb, 0.32 electrons; Te, 0.22 electrons[12]) and allows the amorphous phase to form critical nuclei via forming Sb-Te bonds by small atomic displacements of antimony and tellurium atoms in the

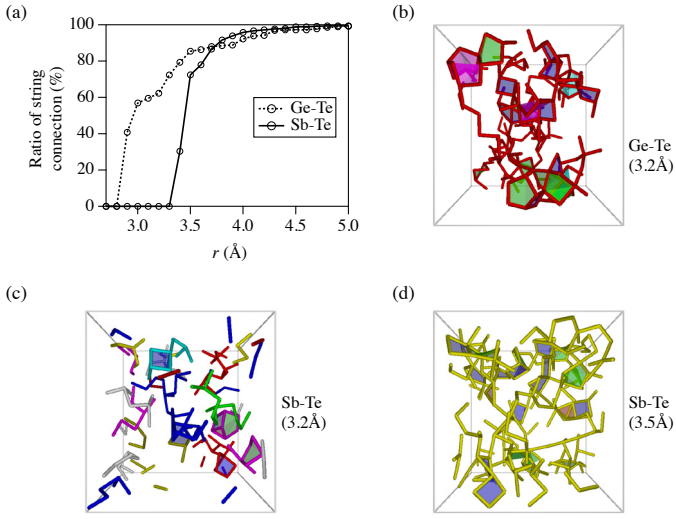

Fig. 3 Atomic configuration and connectivity of Ge-Te and Sb-Te in a-GST obtained by the RMC model. (a) Connectivity of Ge-Te and Sb-Te with different r_{max}. (b) Atomic configuration of Ge-Te (connectivity is considered up to 3.2 Å). (c) Atomic configuration of Sb-Te (connectivity is considered up to 3.2 Å). (d) Atomic configuration of Sb-Te (connectivity considered up to 3.5 Å). The theeefold, fourfold, fivefold, and sixfold rings are highlighted by red, blue, green, and light blue, respectively.

crystallization process. Thus our finding can reasonably explain the reason why the crystallization of a-GST is faster than that of amorphous GeTe in DVD.[13)]

CONCLUSION

We found that germanium forms a covalent core network with tellurium to stabilize the amorphous phase at room temperature, which core network can remain in the crystalline phase. Antimony maintains an atomic ordering with tellurium beyond the Sb-Te covalent bond distance in a-GST; these atomic pairs can rapidly fit into the Ge-Te core network in the crystalline phase at higher temperature induced by a laser irradiation. This behavior is similar to the Sb local environment of distorted 3 + 3 octahedron[4)] found in another phase change material, $Ag_{3.5}In_{3.8}Sb_{75.0}Te_{17.7}$ (AIST), in which Sb possesses locally 3 extra neighbours beyond the nearest coordination covalent bond distance. Our finding can reasonably explain the roles of germanium and antimony in DVD with respect to rapid phase change and durability. Thus it is demonstrated that the observation of network formation is important to reveal the origin of rapid phase change at atomic level. This finding is a crucial new key concept for designing new PC materials with excellent durability.

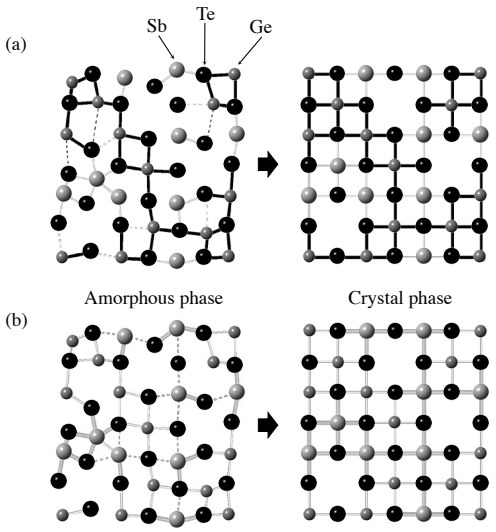

Fig. 4 Schematic drawing showing the phase-change process in a-GST. (a) highlights the Ge-Te core network; (b) highlights the Sb-Te pseudo network. Black colored sticks show Ge-Te bonds up to 3.2 Å. Gray colored sticks show Sb-Te bonds up to 3.2 Å and dotted lines show Sb-Te correlations between 3.2 to 3.5 Å.

ACKNOWLEDGEMENTS

This work was supported by the Japan Science and Technology Agency via the Strategic Japanese-Finland Cooperative Program on “Functional Materials”. LP and LT were partially supported by the Hungarian National Development Agency (NFÜ), via grant No. TÉT_10-1-2011-0004.

REFERENCES

1. M. Wuttig and N. Yamada, Nature Mater. **6**, 824 (2007).
2. D. Lencer, M. Salinga, and M. Wuttig, Adv. Mater. **23**, 2030 (2011).
3. K. Ohara et al., Adv. Func. Mater. **22**, 2251 (2012).
4. T. Matsunaga et al., Nature Mater. **10**, 129 (2011).
5. S. Kohara et al., J. Phys.: Condens. Matter **19**, 506101 (2007).
6. J. Akola et al., Phys. Rev. B **80**, 020201 (2009).
7. S. Kohara et al., Appl. Phys. Lett. **89**, 201910 (2006).
8. O. Gereben, P. Jóvári, L. Temleitner, and L. Pusztai, J. Optoelectron. Adv. Mater. **9**, 3021 (2007).
9. A. Mellergård and R. L. McGreevy, Acta. Cryst. **55**, 783 (1999).
10. L. Guttman, J. Non-Cryst. Solids **116**, 145 (1990).
11. J. Akola, J. Larrucea, and R. O. Jones, Phys. Rev. B **83**, 094113 (2011).
12. J. Akola and R. O. Jones, J. Phys.: Condens. Matter **20**, 465103 (2008).
13. J. H. Coombs, A. P. J. M. Jongenelis, W. v. Es-Spiekman, and B. A. J. Jacobs, J. Appl. Phys. **78**, 4918 (1995).